Talanta 85 (2011) 400–405

Contents lists available at ScienceDirect

Talanta

journal homepage: www.elsevier.com/locate/talanta

Specific O_2^- generation in corona discharge for ion mobility spectrometry

Martin Sabo, Ján Matúška, Štefan Matejčík*

Comenius University, Faculty of Mathematics, Physics and Informatics, Department of Experimental Physics, Mlynska dolina F2, 842 48 Bratislava, Slovakia

ARTICLE INFO

Article history:
Received 13 January 2011
Received in revised form 22 March 2011
Accepted 28 March 2011
Available online 5 April 2011

Keywords:
Ion mobility spectrometry
Corona discharge
Mass spectrometry
Negative ions
Corona wind

ABSTRACT

This study deals with O_2^- generation in corona discharge (CD) in point to plane geometry for single flow ion mobility spectrometry (IMS) with gas outlet located behind the ionization source. We have designed CD of special geometry in order to achieve the high O_2^- yield. Using this ion source we have achieved in zero air conditions that up to 74% all negative ions were O_2^- or $O_2^-(H_2O)$. It has been demonstrated that the non-electronegative nitrogen positively influences the efficiency of O_2^- generation in O_2/N_2 mixtures. The reduced ion mobility of 2.27 $cm^2\,V^{-1}\,s^{-1}$ has been measured for $O_2^-/O_2^-(H_2O)$ ions in zero air. Additional ions detected in zero air (less than 200 ppb CO_2) using the mass spectrometric and IMS technique were, NO_2^-, $N_2O_2^-$ (2.37 $cm^2\,V^{-1}\,s^{-1}$), NO_3^-, $N_2O_3^-$ and $N_2O_3^-(H_2O)$. The CO_3^- and CO_4^- ions have been detected after the introduction of 5 ppm CO_2 into zero air.

1. Introduction

The mass spectrometry investigation of negative ions formation in CD was performed in several studies [1–7]. The type and relative intensities of negative ions yield in these studies differ significantly. This is mainly due to the sensitivity of CD to many parameters like gas composition (air, synthetic air, and impurity level), time period between ion formation and their detection (CD gap dimensions), gas flow and discharge power related to concentration of neutral and radical species in CD gap.

Shahin [1] in his pioneer work detected NO_2^- and NO_3^- as dominant ions in dry air. Gravendeel and Hogg [2] studied negative ion formation in N_2/O_2 mixtures (5:1). They observed numerous negative ions O_3^-, OH^-, NO_3^- and also CO_3^- despite low concentration of CO_2 (0.1 ppm). These results were subsequently contradicted by Gardiner and Cragss [3] who at 1 kPa observed CO_3^- as dominant ion in ambient air. Skalny et al. [4] studied negative ion formation in CD using both wet and dry air CO_3^- and its water clusters as dominant ions. If radicals like ozone and nitrogen oxides were added to CD reactor NO_3^- and its hydrated clusters were formed. Nagato et al. [5] studied the ions formed in different reaction times (1 and 10 ms) in CD. Significant reduction of the ions detected by mass spectrometer was observed with increasing time window. Additionally, decrease of the humidity (25 ppm) resulted in the observation of the NO_3^- as the only ion in the spectrum. Sekimoto and Takyama [6] studied the influence of the CD power on the negative ion formation. For low nominal values of power mainly $OH^-(H_2O)_n$ clusters were detected. The increase of the discharge power resulted in the formation of the large number of negative ions (NO_2^-, NO_3^-, HNO_3^-, CO_3^- and CO_4^-).

The important role of radicals in negative ion formation in CD was pointed out by Ross and Bell [7]. The effective removal of radicals from CD gap by reverse gas flow resulted in the formation of O_2^- and CO_4^- ions.

Implementation of the CD to IMS [8] was introduced as a non-radioactive alternative to widely used radioactive ^{63}Ni [9]. In the positive polarity, the CD due to conversion of primary ions to hydrated protons [10] produces similar positive reactant ions as the radioactive ^{63}Ni. However, the varieties of neutral products and radicals produced in negative CD and formation of very stable negative ions, make exploitation of negative CD in IMS difficult [11]. Several solutions to this problem have been proposed [7,12,13].

Tabrizchi and Abedi [12] proposed implementation of the curtain gas to IMS. This solution is based on non-electronegative nitrogen flow through CD gap. In this case, the negative CD works as source of thermal electrons; these electrons are then injected into reaction region of IMS where the low energy electron attachment to electronegative gas occurs. Non-electronegative gas complicates the implementation of this technique for handheld IMS but for fixed and laboratory analyzers, it can be very useful. Hill and Thomas [13] proposed application of pulsed CD to IMS. This solution exploits the corona wind reduction in the pulsed CD and is associated with lower production of neutrals in the CD gap. In this case, however, additional electronics is required. Ross and Bell [7] proposed the solution based on the reverse flow continuous CD in wire to cylinder (or double wings, specification was not given) geometry.

* Corresponding author. Tel.: +421 260295686; fax: +421 65429980.
E-mail address: matejcik@fmph.uniba.sk (Š. Matejčík).

0039-9140/$ – see front matter © 2011 Elsevier B.V. All rights reserved.
doi:10.1016/j.talanta.2011.03.074

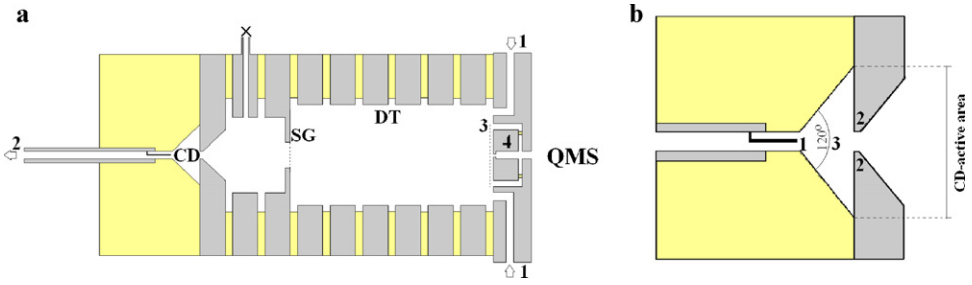

Fig. 1. (a) Schematic view of single flow IMS: 1 – gas inlet, 2 – gas outlet, 3 – aperture grid, 4 – ion collector; (b) CD reactor 1 – tip electrode, 2 – target electrode, 3 – CD gap.

In this case, the neutrals formed in CD gap are removed out of the active region by the reverse flow, so that the neutral products and radicals cannot enter into the reaction and the drift tube. This technique requires additional gas flow.

In this study the generation of O_2^- is studied in single flow IMS equipped with CD in simple point to plane geometry. We discuss the O_2^- generation in O_2 and O_2/N_2 mixtures as a function of CD gap and gas flow. At optimal discharge gap and gas flow the O_2^- yield of 74% has been achieved. In the paper we discuss the formation of isobaric ions CO_3^- and $N_2O_2^-$ and CO_4^- and $N_2O_3^-$ in air.

2. Experiment

Home built single flow IMS (Fig. 1a) was used in our experiment. The IMS was built from nine stainless steel ring electrodes isolated by Teflon rings. The electrodes were supplied from the divider where the last electrode was connected through a resistor to grounded plate. The spectrometer was equipped with CD ion source in simple point to plane geometry (Fig. 1b). The gas outlet was located behind the corona thus the CD operated at so-called reverse flow regime. The orifice between the CD region and reaction region of IMS was designed in such way that the neutral products of CD are effectively removed from this region into exhaust [14,15]. The CD needle was made from tungsten wire with diameter 150 μm and was located in front of target electrode with an orifice with diameter of 3 mm. The CD gap was operated at three different distances: 3, 5 and 7 mm. The corona current was set to 6 μA in all experiments. The distance between the plane electrode of the CD and shutter grid (SG) was 3.8 cm while the drift region length was 8.2 cm. The Bradbury–Nielsen type of SG was located at the third electrode. The SG was manufactured from tungsten wires with diameter 50 μm at 0.5 mm separation. The opening time of SG in present experiment was 50 μs. The ion collector was shielded by aperture grid with transmittance 88%. The ion current was processed by current to voltage amplifier 5×10^8 V/A (FEMTO Messtechnik) and the IMS spectra have been recorded by AD card (Picoscope). Two high-voltage power supplies (Heinzinger LNC 1000) were used, one for corona discharge and one for drift field of IMS (500 V/cm). The SG was controlled by fast high-voltage transistor switch (Behlke Electronic GMH, HTS 21-14) and triggered by TTL generator. The IMS was operated at ambient temperature of 295 K maintained by air conditioning. The pressure was recorded by high sensitive gauge (PFEIFFER CMR 361). The calculated deviation in the determination of the mobilities of the ions was 2%.

The IMS was interfaced to quadrupole mass spectrometer (QMS) described in our previous paper [16]. The QMS was operated in two modes. In full scan mode the SG of IMS was fully open and the mass spectra of ions present in the drift tube were recorded. The typical mass to charge ratio (m/z) range in this mode was from $m/z = 30$ to $m/z = 120$ with 5 s scan for one m/z. Second mode of operation was "mass resolved IMS mode" where the QMS was set to certain value of m/z and the IMS spectrum was recorded using mass spectrometer.

The gases used in this experiment were oxygen, nitrogen of 5.0 purities (99.999% LindeGas) and carbon dioxide of 5.6 purity (99,9996% Linde Gas). The digital mass flow controllers (MKS Instruments) were used to prepare mixtures of the gases.

3. Results and discussion

The ion mobility spectra recorded in oxygen for several CD gaps in dependence on the oxygen flow 700, 1000 and 1200 ml/min are presented in Fig. 2. The dominant peak with reduced ion mobility of 2.52 $cm^2\ V^{-1}\ s^{-1}$ of m/z was in our previous study [16] assigned to $N_2O_2^-$. In addition to this peak we have observed additional peak with reduced mobility of 2.44 $cm^2\ V^{-1}\ s^{-1}$ at gas flow 1200 ml/min. The mass spectrometric analysis showed that this peak corresponds to $O_2^-(H_2O)_{0.1}$ [17]. The presence of this peak in the mobility spectrum is due to more effective removal of the reactive neutral products from CD gap at elevated gas flow [7]. It is also evident from Fig. 2, that the highest yield of O_2^- anions was achieved at 5 mm CD gap, while at other distances was this yield close to limit of detection of the IMS. The O_2^- yield of 13% of the total ion yield was achieved in pure oxygen at 1200 ml/min gas flow, corona current 6 μA and the tip distance 5 mm. It would be possible to some extent to increase the efficiency of O_2^- generation in pure oxygen, by decreasing the corona discharge current and increasing the oxygen flow. We have achieved up to 20% of O_2^- yield in our laboratory by increasing the oxygen flow to 2 l/min and decreasing the CD current to 4 μA. However, further increase of the gas flow did not result in higher O_2^- yield.

Different situation occurs when the gas composition is changed from O_2 to O_2/N_2 mixture. The mobility spectrum for O_2/N_2 mixture with nitrogen concentration 0%, 20%, 50% and 80% (zero air) at total gas flow 1000 ml/min is given in Fig. 3. It is evident from this figure that with the increasing nitrogen concentration the $O_2^-/O_2^-(H_2O)$ yield is increasing. We suppose that this positive effect is due to thermalisation of the electrons in the CD gap by nitrogen and thus reduction of the dissociation of the molecules by electron impact or dissociative electron attachment to O_2. The low energy electrons are in next step attached in three body reaction to oxygen [18]:

$$(1)\ e^- + O_2 + M \rightarrow O_2^- + M$$

where $M = O_2$ or N_2. The evolution of O_2^- in dependence of nitrogen concentration for three different discharge gaps is depicted in Fig. 4. In analogy to pure oxygen the most effective O_2^- yield was at 5 mm point to plane distance while the worst case was achieved at 7 mm distance. These differences in efficiency of O_2^- production as a function of the CD gap we attribute to the corona wind. The direction of the corona wind in CD is from point to plane electrode to plane electrode [15]. This wind counteracts to the gas flow and thus increases the transport of the neutrals from the CD to the reaction region of IMS. The increase of the CD gap leads to stronger electric wind generation [15]. This is the reason why the O_2^- yield is weak at large CD gaps. However, decreasing the CD gap leads to discharge concentration in front of the needle and velocity profile

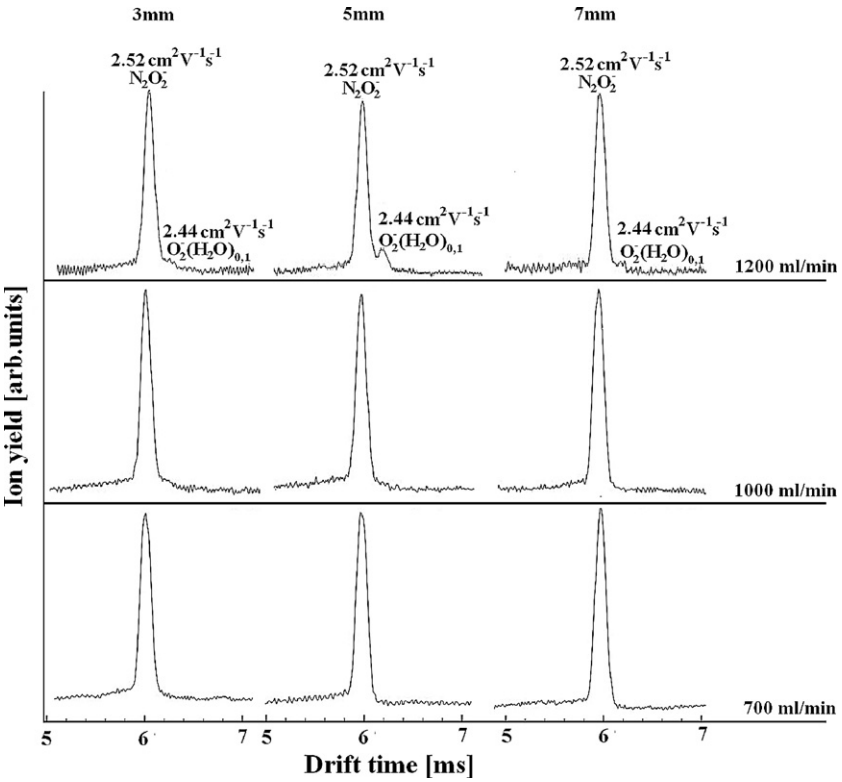

Fig. 2. The IMS spectra in pure oxygen for gas flow 700, 1000 and 1200 ml/min and for different point to plane gaps. The peaks with reduced mobility 2.52 $cm^2\ V^{-1}\ s^{-1}$ and 2.44 $cm^2\ V^{-1}\ s^{-1}$ were mass spectrometrically assigned to $N_2O_2^-$ ($m/z = 60$) and to $O_2^-/O^-(H_2O)$ ($m/z = 32$ and 50).

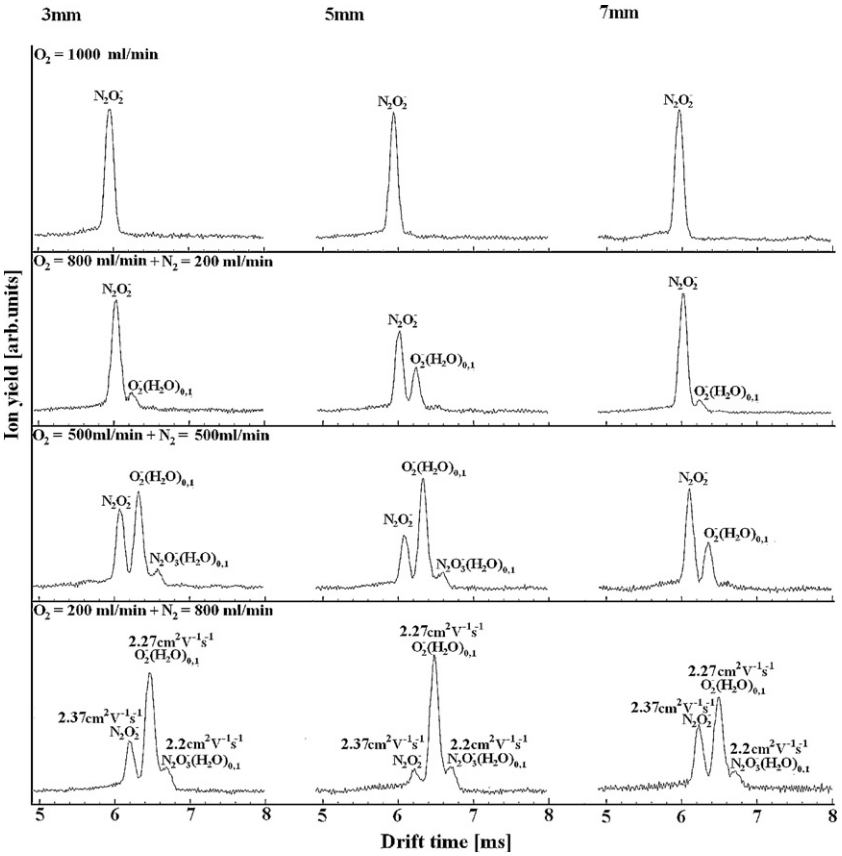

Fig. 3. The IMS spectra for O_2/N_2 mixtures with nitrogen concentrations 0%, 20%, 50% and 80% (zero air) at total gas flow 1000 ml/min for different point to plane gaps. The assignment of IMS peaks was carried out on the basis of mass spectrometrically resolved IMS.

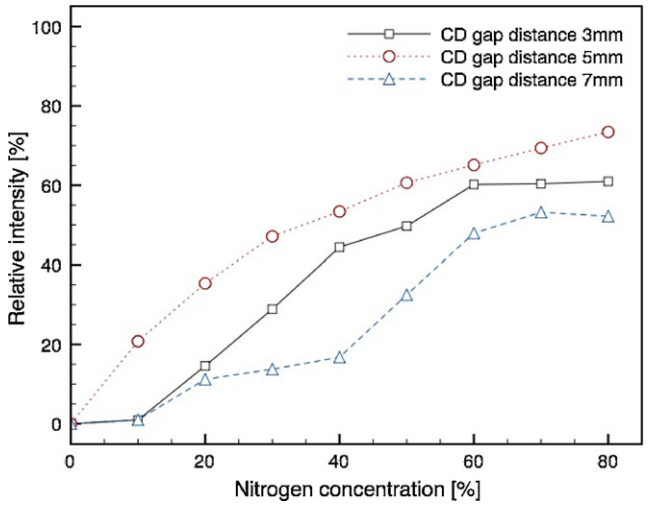

Fig. 4. Evolution of O_2^- yield for nitrogen concentration from 0% to 80% for different point to plane geometries.

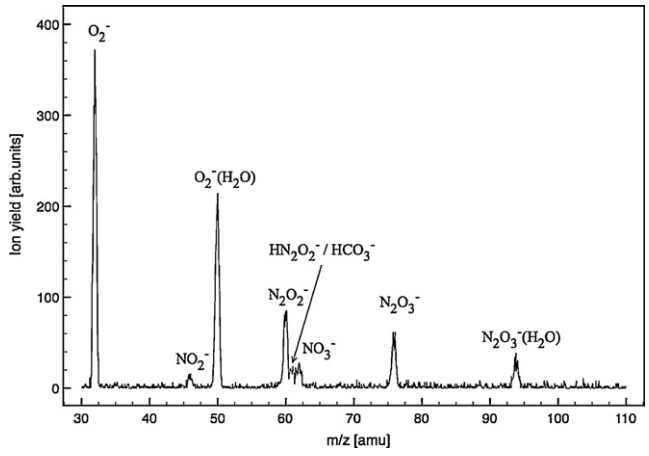

Fig. 5. The mass spectrum of negative CD in zero air measured at point to plane distance 5 mm and opened shutter grid of IMS.

of corona wind is thinner, which again results in higher velocity of the corona wind [15]. For this reason O_2^- yield at 3 mm CD gap is lower than at 5 mm as seen in Fig. 4. The best O_2^- yield (74% of total ion yield) was achieved at O_2/N_2 mixture in zero air for CD gap of 5 mm. The mass spectrum measured in synthetic air at 5 mm CD gap (with opened SG) is depicted in Fig. 5. The dominant ions observed in mass spectrum are O_2^- ($m/z = 32$), $O_2^-(H_2O)$ ($m/z = 50$) and $N_2O_2^-$ ($m/z = 60$). The calculated reduced mobility of $N_2O_2^-$ in zero air is 2.37 $cm^2\,V^{-1}\,s^{-1}$ while the reduce mobility of dominant peak is 2.27 $cm^2\,V^{-1}\,s^{-1}$. The dominant peak was composed of O_2^- and $O_2^-(H_2O)$ due to their drift in thermodynamic equilibrium. The mass resolved analysis of IMS spectrum is depicted in Fig. 6a.

It is generally accepted that in IMS the ions and their clusters drift in thermodynamic equilibrium. The thermodynamic equilibrium is established on the basis of formation and decay of cluster ions. However, if the stability of the cluster ions exceeds substantially that of the parent ions, then the cluster ions are able to drift independently of parent ions. The example for the common drift of the parent ions with the cluster ions in thermodynamics is system $O_2^-/O_2^-(H_2O)_n$. Watts [19] observed that the ions $O_2^-(H_2O)_{0,1}$ and $CO_4^-\cdot(H_2O)_{0.1}$ ($O_2^-\cdot CO_2\cdot(H_2O)_{0.1}$) do not drift in thermodynamic equilibrium. This observation was now confirmed by the mass resolved IMS spectrum in Fig. 6a, where the ions with $m/z = 76$ and their water clusters $m/z = 94$ appear at different drift times than the $O_2^-(H_2O)_{0,1}$ ions. In order to verify the statement of Watts [19] we have increased the zero air flow up to value 2000 ml/min. This resulted in an reduction of $N_2O_2^-$ in IMS spectrum at the expense of $O_2^-(H_2O)_{0,1}$ (Fig. 6b). The mass resolved ion mobility spectrum measured at $m/z = 76$ exhibits two peaks as it is depicted in Fig. 6b. The two peaks of $m/z = 76$ indicate existence of the two different ions with $m/z = 76$. One of them we assign to CO_4^- the other one to $N_2O_3^-$ [20] which has an appreciable electron affinity of 2.43 eV [21]. In order to distinguish between these isobaric ions we have seeded 1000 ml/min zero air with 5 μl/min of CO_2 (5 ppm CO_2 concentration). The corresponding mass spectrum is presented in Fig. 8. The addition of CO_2 resulted in the increase of CD current to 12 μA and in changes in the IMS spectrum (Fig. 7a). The value of the reduced ion mobility of the dominant peak (mixture of $O_2^-(H_2O)_{0,1}$ ions) changed from 2.27 $cm^2\,V^{-1}\,s^{-1}$ to 2.20 $cm^2\,V^{-1}\,s^{-1}$. The mass resolved IMS revealed additional two ions within this IMS peak ($m/z = 60$ and $m/z = 76$). The other IMS peaks were as well identified using the mass resolved IMS spectra. The peak with reduced ion mobility of 2.27 $cm^2\,V^{-1}\,s^{-1}$ consists of ions with $m/z = 76$ and the peak with reduced ion mobility 2.37 $cm^2\,V^{-1}\,s^{-1}$ consists of ions with $m/z = 60$. We have assigned ions with $m/z = 76$ and reduced mobility 2.27 $cm^2\,V^{-1}\,s^{-1}$ to CO_4^-, and the ions with reduced mobility 2.20 $cm^2\,V^{-1}\,s^{-1}$ to $N_2O_3^-$. This assignment is in agreement with data presented by Watts [19] who at similar conditions (4 ppm of H_2O and CO_2) observed the CO_4^- ions in IMS at different drift times than the $O_2^-(H_2O)_n$ ions. In his experiment radioactive ^{63}Ni ion source was used in which the formation of $N_2O_3^-$ was negligible. Concerning the nature of the ions with $m/z = 60$, the experiment with admixture of CO_2 indicated that the ion with reduced ion mobility of 2.37 $cm^2\,V^{-1}\,s^{-1}$ is $N_2O_2^-$, while the CO_3^- has in zero air reduced ion mobility of 2.20 $cm^2\,V^{-1}\,s^{-1}$.

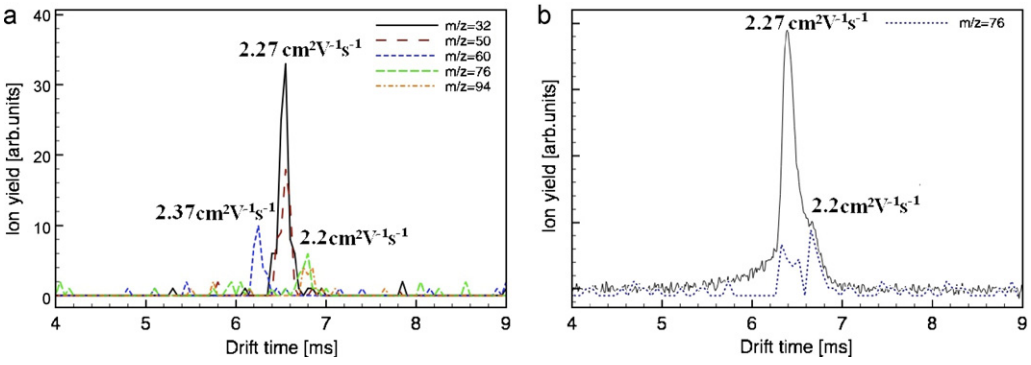

Fig. 6. (a) Mass resolved ion mobility spectrum measured at point to plane gap of 5 mm in zero air flow 1 l/min and (b) IMS spectrum measured at point to plane gap of 5 mm in zero air flow 2 l/min and corresponding mass resolved IMS spectrum measured at $m/z = 76$.

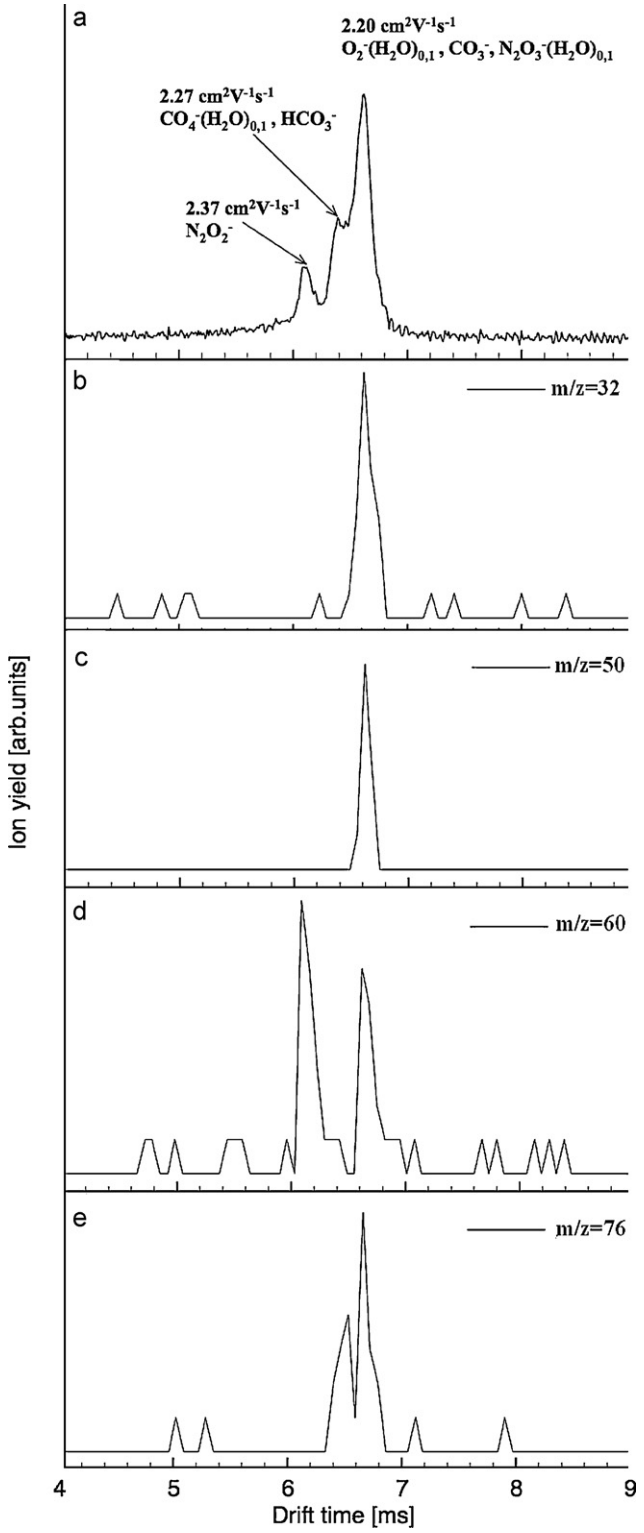

Fig. 7. (a) IMS spectrum measured in zero air with 5 ppm CO_2 at total gas flow 1 l/min. The mass resolved mobility spectra of most abundant ions of (b) $m/z = 30$, (c) $m/z = 50$ (d) $m/z = 60$ and (e) $m/z = 76$.

The nature of the ions with $m/z = 60$ in nitrogen was also discussed by Ewing and Waltman [22]. They used nitrogen (99.999% purity) with 0.25% admixture of ^{18}O labelled oxygen (95% purity). The presence of CO_3^- in their spectrum was confirmed. This result was assigned to the diffusion as a possible source of CO_2 in their experiment. In our former study [17] of high purity oxygen

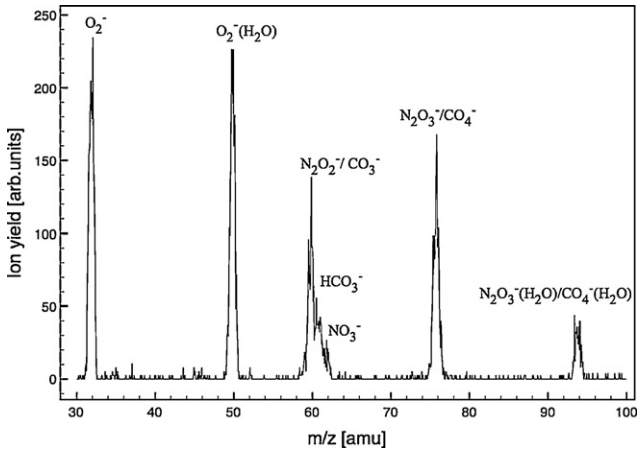

Fig. 8. Mass spectrum measured in zero air with 5 ppm CO_2 and total gas flow 1 l/min when the SG of IMS was fully open.

(99.9999%), the dominant ion with $m/z = 60$ has been detected and it has been assigned to $N_2O_2^-$. The formation of this ion was associated with N_2 as a main impurity in high purity oxygen. When the concentration of CO_2 was increased to 200 ppb, CO_3^- was detected, however, at lower intensities.

In the mass spectrum measured in zero air (Fig. 5) negative ions with $m/z = 46$ and $m/z = 62$ were detected. These ions were attributed to NO_2^- ($m/z = 46$) and to NO_3^- ($m/z = 62$) which are known to be stable negative ions in dry air [4]. Due to increase of relative yield of peak with $m/z = 61$ after the addition of CO_2 (Fig. 8) we have assigned this ion to HCO_3^- [5] with reduced mobility 2.27 $cm^2\,V^{-1}\,s^{-1}$.

The addition of CO_2 to zero air in present experiment resulted in significant increase of CD current. The increase of CD current resulted in higher radical formation in CD gap [6,17] and had significantly affected the ion yield. On the other hand, the injection of lower CO_2 admixtures was not possible due to limitation of the available mass flow controllers. For this purpose we were not able to quantify the dependence between $N_2O_2^-$ and CO_3^- as well like those between CO_4^- and $N_2O_3^-$ in the experiment, this quantification will require additional studies.

4. Conclusion

In this study the negative CD ion source for single flow IMS was proposed. The CD reactor was designed in order to reduce unwanted corona wind and the transport of neutral reactive species from CD into reaction region of the IMS spectrometer and to maximise the O_2^- production in the CD ion source. We have observed that the yield of O_2^- in O_2/N_2 mixture and zero air was higher than in pure O_2. We attributed this behaviour to efficient thermalisation of electrons in collision with nitrogen and thus lower dissociation of the ions and molecules in the CD. The 73.5% of O_2^- yield in zero air was achieved for 5 mm CD gap. In order to understand in detail the processes in the CD, 5 ppm of CO_2 has been added to the zero air. In the IMS and MS spectra $N_2O_3^-$, CO_4^- ($m/z = 76$), $N_2O_3^-\cdot(H_2O)$ ($m/z = 94$) and $N_2O_2^-$, CO_3^- ($m/z = 60$) ions have been identified and the values of the reduced ion mobilities for these ions have been determined.

Acknowledgements

This work was supported by the Slovak research and development agency Projects LPP-06-0146 and the VEGA Grant 1/0379/11. Authors would like to dedicate this study to the memory of Professor Ján Dušan Skalný.

References

[1] M. Shahin, Appl. Opt. Suppl. Electrophotogr. 3 (1969) 106.
[2] B. Gravendeel, F.J. Hoog, J. Phys. B: At. Mol. Phys. 20 (1987) 6337.
[3] P.S. Gardiner, J.D. Cragss, J. Phys. D: Appl. Phys. 10 (1977) 1003.
[4] J.D. Skalny, T. Mikoviny, S. Matejcik, N.J. Mason, Int. J. Mass Spectrom. 233 (2004) 317.
[5] K. Nagato, Y. Matsui, T. Miyata, T. Yamauchi, Int. J. Mass Spectrom. 248 (2006) 142.
[6] K. Sekimoto, M. Takayama, Int. J. Mass Spectrom. 261 (2007) 38.
[7] S.K. Ross, A.J. Bell, IJMS 218 (2002) L1–L6.
[8] M. Tabrizchi, T. Khayamian, N. Taj, Rev. Sci. Instrum. 71 (2000) 465.
[9] G.A. Eiceman, Z. Karpas, Ion Mobility Spectrometry, 2nd ed., CRC Press, 2005.
[10] M. Pavlik, J.D. Skalny, Rapid Commun. Mass Spectrom. 11 (1997) 1757.
[11] R.G. Ewing, M.J. Waltman, Int. J. Ion Mobil. Spec. 12 (2009) 65.
[12] M. Tabrizchi, A. Abedi, Int. J. Mass Spectrom. 218 (2002) 75.
[13] C.A. Hill, C.L.P. Thomas, Analyst 128 (2003) 55.
[14] R.S. Sigmond, J. Appl. Phys. 53 (1982) 891.
[15] E. Moreau, G. Touchard, J. Electrostat. 66 (2008) 39.
[16] M. Sabo, J. Páleník, M. Kučera, H. Han, H. Wang, Y. Chu, Š. Matejčík, Int. J. Mass Spectrom. 293 (2010) 23.
[17] M. Sabo, Š. Matejčík, Anal. Chem. 83 (2011) 1985.
[18] J.L. Pack, A.V. Phelps, J. Chem. Phys. 44 (1965) 1870.
[19] P. Watts, Int. J. Mass Spectrom. Ion Processes 121 (1992) 141.
[20] A.K. Luong, T.G. Clements, R.E. Continetti, Int. J. Mass Spectrom. 220 (2002) 253.
[21] M. Chen, M. Zhou, Q. Qin, Chem. Phys. Lett. 321 (2000) 498.
[22] R.G. Ewing, M. Waltman, Int. J. Mass Spectrom. 296 (2010) 53.